Structural phase transitions in malononitrile, $CH_2(CN)_2$: crystal structure of the δ phase by neutron powder diffraction, and ab initio calculations of the structures and phonons of the α and δ phases

Lei Tan

Department of Physics and Astronomy, Queen Mary University of London, Mile End Road, London, E1 4NS, UK.

Keith Refson

Department of Physics, Royal Holloway University of London, Egham Hill, Egham, Surrey, TW20 0EX, UK, and
ISIS facility, Harwell Campus, Didcot, OXON OX11 0QX.

Martin T Dove

Department of Physics, School of Sciences, Wuhan University of Technology, 205 Luoshi Road, Hongshan district, Wuhan, Hubei, 430070, People's Republic of China and
Department of Physics and Astronomy, Queen Mary University of London, Mile End Road, London, E1 4NS, UK

E-mail: martin.dove@qmul.ac.uk

Abstract. The crystal structure of the low-temperature δ phase of crystalline malononitrile, $CH_2(CN)_2$ (stable phase below 260 K), has been determined using Rietveld refinement on neutron powder diffraction data. The δ phase has a slightly lower density than the other three low-pressure phases, and unlike those phases it has a polar structure. The transition from the β to δ phase involves a major reconstruction of the structure, including establishing a network of hydrogen bonds. DFT simulations of the structure and phonon dispersion curves of both α and δ phases give free energy curves consistent with the phase transitions. It is noted that the transition from the δ to β phase at 260 K is facilitated by the entropy arising from the low-frequency phonons associated with the soft mode for the sequence of α–β–γ phase transitions.

Submitted to: *J. Phys.: Condens. Matter*

1. Introduction

The existence of phase transitions in crystalline malononitrile, $CH_2(CN)_2$, were first identified by ^{14}N nuclear quadrupole resonance measurements [1, 2] and through measurements of the heat capacity [3]. These measurements identified second-order displacive phase transitions at 141 and 295 K on fast cooling from high temperature, and a first-order reconstructive phase transition at 260 K on slow cooling.‡ Malononitrile can be easily supercooled below the reconstructive phase transition. The startling feature of the sequence of displacive phase transitions is that the low-temperature α phase and high-temperature γ phase share the same crystal structure (space group $P2_1/n$), with the intermediate-temperature β phase having lower symmetry (space group $P\bar{1}$) [4, 5]. Measurements by neutron powder diffraction of the variation of the crystal structure, and hence of the order parameter and coupled symmetry-breaking strains, have recently been reported [5]. Such a sequence of phase transitions, called 're-entrant phase transitions', are very uncommon; the best other example is the paraelectric–ferroelectric–paralectric phase transition in Rochelle Salt [6]. The phase transitions were also investigated as a function of pressure using Raman spectroscopy [7], finding a new high-pressure phase. The phase diagram is shown in Figure 1. The outstanding questions in the study of the phase transitions in malononitrile now concern the crystal structures of the ambient-pressure δ phase and of the new high-pressure phase [7]. In this paper we report a solution of the crystal structure of the δ phase by neutron powder diffraction. The results are supported by ab initio calculations of the structures, energies and phonon frequencies of the δ and α phases.§ As a result we have added a tentative phase boundary line for the stability field of the δ phase to the phase diagram in Figure 1. We also used ab initio lattice dynamics simulations to search for an instability associated with the high-pressure phase transition, but no indication was found.

There have been two previous, but inconclusive, x-ray powder diffraction studies of δ-malononitrile [8, 9]. These showed drastic changes in the diffraction patterns, consistent with a reconstructive phase transitions. However, it was not possible to index the diffraction patterns, in part perhaps because it was clear that some peaks were doublets [9]. The NQR results showed that there is only one independent crystallographic position for the N atom. A spectroscopic study of the four ambient-pressure phases of malononitrile using partial deuteration [10] showed two distinct C–D vibrations in the α and γ phases, and three in the β phase, consistent with 2 or 4 symmetrically distinct sites for the hydrogen atoms. Based on an asymmetric peak shape for the C–D vibration band in the δ phase it was suggested that there are two symmetrically distinct hydrogen sites in the δ phase; we will discuss this point below.

‡ The results of the calorimetric study [3] had been interpreted into terms of a possible second-order λ-type anomaly associated with an order–disorder phase transition at 260 K, but all subsequent work is inconsistent with such an interpretation.

§ It should be noted that other authors have denoted the α, β, γ and δ phases as IV, II, I and III, or as T′, F, T and L, respectively. The nomenclature with Greek characters used here and in earlier papers [4, 5] better reflects the re-entrant sequence.

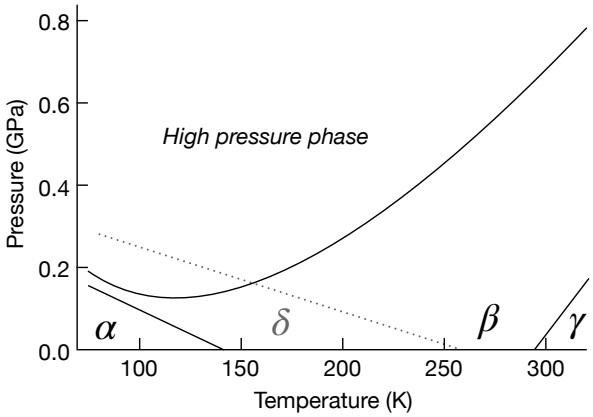

Figure 1. Pressure-temperature phase diagram for the five known crystalline phases of malononitrile. The solid lines represent the phase diagram determined for the α, β, γ and new high-pressure phase determined by Krauzman et al. [7]. Based on the new crystal structure reported here, and the experimental determination of entropy [3], we have estimated the phase boundary line for the thermodynamic stability of the δ phase, shown as the dotted line. The slope was determined from the standard thermodynamic identify $\mathrm{d}P/\mathrm{d}T = \Delta S/\Delta V$, where ΔS and ΔV and the differences in entropy and volume respectively between the δ and β phases. The negative slope of the δ phase boundary arises because of its lower density relative to the other low-pressures phases.

In the recently reported study of malononitrile by neutron powder diffraction [5] the δ phase was produced accidentally by maintaining the sample at a temperature just below 260 K. The lattice parameters determined from an automatic indexing procedure following by refinement using the Le Bail method [11] were given in the report of that study [5]. The crystal structure has subsequently been solved and refined by the Rietveld method, and is reported here. The structural findings here are further investigated using Density Functional Theoretical calculations of structure and lattice dynamics for both α and δ phases.

2. Neutron powder diffraction

2.1. Methods and data analysis

As noted above, the data described in this paper were collected as part of our recently-reported neutron powder diffraction study, and technical details are described there. Briefly, a commercial hydrogenous sample of malononitrile was purifed by distillation, ground into a powder, and placed into a vanadium can. Measurements were made on the D1A diffractometer at the Institute Laue Langevin [12], with neutron beam wavelength of 1.909 Å. Temperature was controlled by a standard helium-flow cryostat. Data were collected for a range of scattering angles from 10–156°. Data reported in this paper were collected at a nominal temperature of 260 K.

Rietveld analysis was performed using the GSAS code [13] through the EXPGUI

interface [14]. Data from different detectors were not merged, but instead were treated as separate data sets. The Bragg peak profiles were described using the standard Gaussian profile with an asymmetry correction (GSAS line profile 1 [13]). The peak widths were represented by the standard three parameters U, V and W [15]; the values of these line-width parameters were constrained to be the same for each set of data in the refinement. A zero-offset on the 2θ angle was refined separately for each data set. The background within each diffraction pattern was modelled using a cosine Fourier function (GSAS background type 2 [13]) polynomials with five refineable parameters.

The lattice parameters from automatic indexing suggested a tetragonal cell. By using the Le Bail method [11] it was quickly shown that the lattice is body-centred tetragonal, and inspection of absent reflections initially suggested space group $I4_1/acd$, but this has too much symmetry. A number of space groups were explored with atomic positions proposed by hand using CrystalMaker visualisation software [16]. The model that was immediately consistent with data has space group $I4_1cd$. The symmetry meant that the central carbon atom has no fractional coordinates to refine, and it was only necessary to refine the fractional coordinates of one other C, N and H atom. The quality of the data was such that the refinement did not require the use of restraints on the molecular bond lengths or angles.

2.2. Results

The trial crystal structure with space group $I4_1cd$ was able to fit the experimental diffraction patterns well, as can be seen in Figure 2. The overall profile R-factor with background subtraction was 2.7% (that is, summed over all data sets), and the overall weighted R-factor (also with background subtraction) was 3.2%, with an overall χ^2 value of 1.15. All the peaks in the diffraction patterns were accounted for, and in the lower-angle region of the diffraction pattern where peak overlap is slight (up to $2\theta = 80^\circ$) there were only four Bragg peaks where the intensity of the Bragg peak (both experimental and calculated) is less than the level of noise in the data. The refined crystal structure is shown in Figure 3, and structural parameters are reported in Table 1. Selected bond lengths and angles are given in Table 2 and are consistent with standard values.

The crystal structure of δ-malononitrile is polar. The central C atoms lie on the crystal 2-fold axes, and the molecular 2-fold axes are coincident with the crystal 2-fold axes. Thus all molecules have their dipole moments parallel to the crystallographic z axis. In addition to refining the atomic coordinates, values of isotropic temperature factors were also refined, and given in Table 1. Because no attempt was made to take account of beam attenuation, the absolute values of the refined parameter values may be subject to a systematic shift towards lower values, but the relative sizes for the different atoms are reasonable

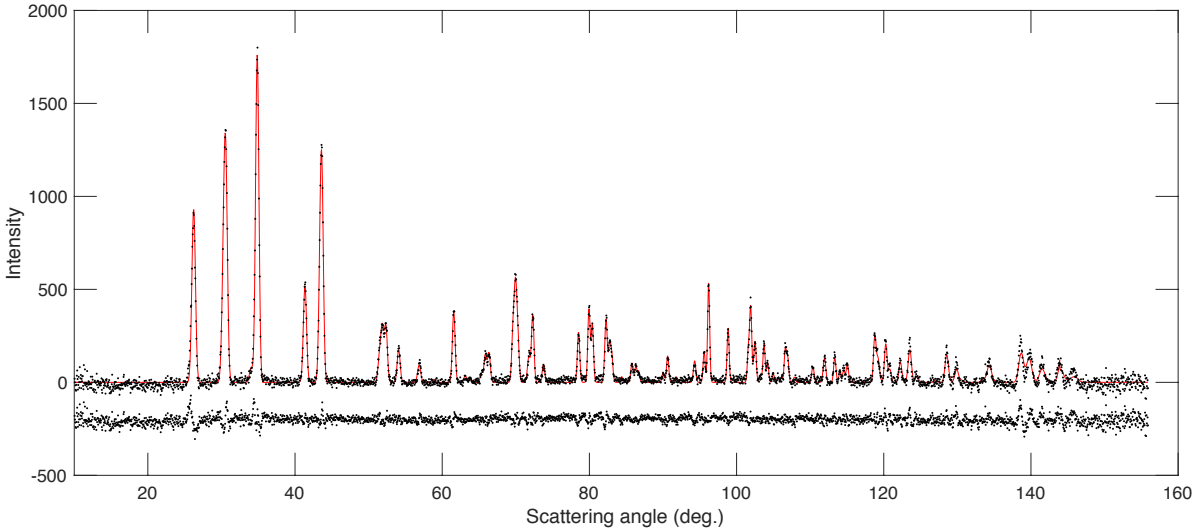

Figure 2. [color online] Comparison of measured (points) and fitted (red curve) diffraction pattern from δ-malononitrile at temperature of 260 K (background subtracted). The difference between the two is shown as the lower curve. This figure was constructed by merging the 10 data sets for the different detectors, although these were treated separately in the actual analysis.

Table 1. Crystal structure of the δ phase of malononitrile (space group $I4_1cd$) from experiment at a temperature of 260 K (top line in each atom entry) and from DFT calculations (bottom line in each atom entry, section 3.2). Experimental lattice parameters are $a = 7.2918(2)$ Å and $c = 14.4455(4)$ Å, and from DFT energy minimisation are $a = 7.10009$ Å and $c = 14.0572$ Å. Atomic coordinates are given as fractional values. Estimated errors in the last significant figures of the experimental data are given in brackets. C1 has the same coordinates in both experiment and DFT; symmetry allows the value of the z coordinate to be arbitrary.

Atom	x	y	z	$u_{\rm iso}$ (Å^2)
C1	0	0	0	0.035(3)
C2	0.101(1)	0.124(1)	0.056(1)	0.030(2)
	0.1130	0.1271	0.0582	
N	0.1950(8)	0.2241(9)	0.1009(7)	0.047(2)
	0.2035	0.2294	0.1036	
H	0.083(3)	−0.081(3)	−0.0430(15)	0.055(4)
	0.09350	−0.0836	−0.04638	

2.3. Discussion of the crystal structure of δ-malononitrile

The crystal structure of δ-malononitrile has much higher symmetry than the other ambient-pressure phases, and a density that is 5% lower. Unlike the α, β and γ phases the crystal structure of the δ phase is polar. The crystal structure is consistent with the NQR results [1, 2], which indicated that all nitrogen atoms within the unit cell occupy symmetrically equivalent sites. Savoie et al [10] have suggested, based on a measurement of C–D stretching vibrations in partially deuterated $CHD(CN)_2$ molecules, that the two

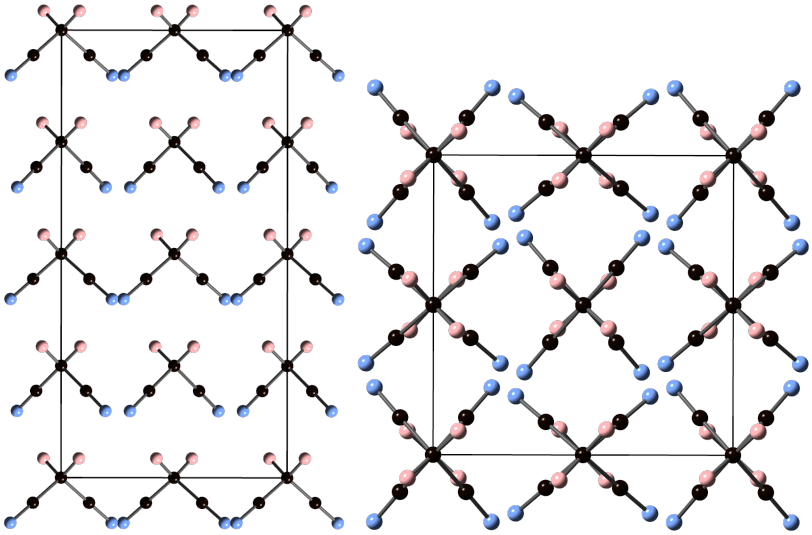

Figure 3. [color online] Two views of the crystal structure of the δ phase of malononitrile at temperature around 260 K, viewed down the a (left) and c (right) axes. In both views the origin of the unit cell is in the bottom-left corner, and the x axis runs from right to left. Carbon atoms are black, nitrogen blue, and hydrogen pink. Image produced using CrystalMaker software [16]

Table 2. Selected bond lengths and angles of the malononitrile molecule in the δ phase. Top line, with standard deviation in the last figure given in brackets, is from the experimental crystals structure, and second line is from the results of the DFT calculations (section 3.2).

C–C	C–N	C–H	C–C–C	H–C–H	C–C–N	C–C–H
1.46(1) Å	1.16(1) Å	1.05(2) Å	112.5(9)°	107(2)°	179.1(9)°	111(1)°, 107(1)°
1.4589 Å	1.1609 Å	1.1037 Å	111.77°	107.57°	179.24°	109.24°, 109.46°

hydrogen atoms within the molecule occupy symmetrically different sites, and thus they proposed that the CH_2 group lies within mirror planes in the crystal structure which might give rise to the equivalence of the sites containing nitrogen atoms. However, the space group $I4_1cd$ does not contain mirror planes, and the structure has equivalent sites for the hydrogen atoms. We note, however, that the splitting of the C–D infrared band that was cited as evidence for the inequivalent hydrogen sites is tiny compared to the splitting in other phases, and only appears as the existence of a shoulder in a peak. The likelihood is that the shoulder reported by Savoie et al [10] is no more than a small artefact, possibly associated with the rapidly varying background, and is not a true peak splitting and hence not really an indicator of symmetry proposed by these authors.

One significant difference between the crystal structures of the δ phase and the other ambient-pressure phases concerns the C–H...N linkages. These are compared in Figure 4. In the α phase each hydrogen atom is virtually equidistant from the nitrogen atoms in two neighbouring molecules (approximate distance is 2.5 Å) without the C–H bond pointing towards any particular atom. On the other hand, in the δ phase each

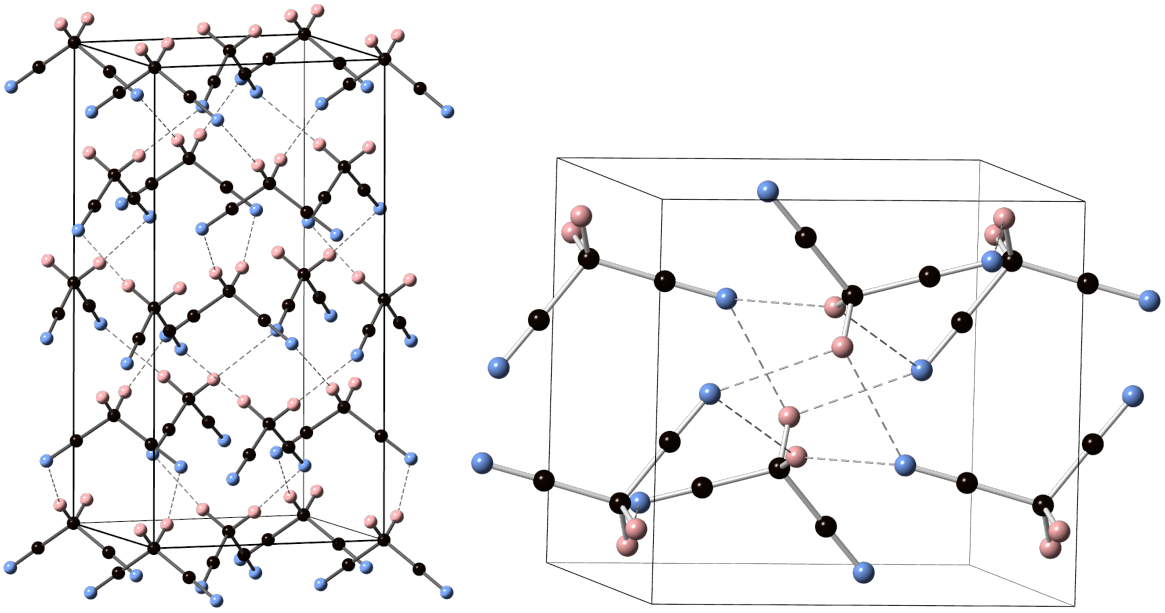

Figure 4. [color online] Comparison of the C–H...N linkages (dashed lines) in the δ (left) and α (right) phases of malononitrile. Carbon atoms are black, nitrogen blue, and hydrogen pink. Image produced using CrystalMaker software [16]

C–H bond clearly points towards one specific nitrogen molecule, with the C–H ...N angle at 167°, a nearly-linear alignment characteristic of hydrogen bonds. The H ...N distance is not significantly shorter in the δ phase, but is within the range of hydrogen bond lengths found in organic materials. The distance is 2.47 Å in the refined crystal structure.

3. Density Functional Theory calculations

3.1. Methods

Density Functional Theory calculations on the crystal structures and lattice dynamics of malononitrile were performed using the CASTEP code [17], using the Grimme semi-empirical correction for the dispersion interaction [18], and linear response density functional perturbation theory for the vibrational dynamics [19]. The generalised gradient approximation (GGA) with the Perdew-Burke-Ernzerhof (PBE) functional [20] was used, in conjunction with norm-conserving pseudopotentials. The cut-off energy was chosen at 1200 eV on the basis of convergence tests. The electronic states with the Brillouin zone were sampled on a $2 \times 2 \times 2$ Monkhorst-Pack grid [21] for all calculations. Residual forces on atoms after energy relaxation were less than 0.001 eV Å^{-1}. Dispersion curves were drawn using our own software package [22].

Table 3. Comparison of the crystal structure of the α phase of malononitrile (space group $P2_1/n$) from the DFT calculations reported here (right columns) and experiment at a temperature of 5 K (left columns, [5]). Experimental lattice parameters are a = 7.81624(9) Å, b = 7.4227(1) Å, c = 6.01624(9) Å, β = 99.394(1)°, and from DFT energy minimisation are a = 7.735 Å, b = 7.416 Å, c = 5.969 Å, and β = 100.14°. Atomic coordinates are given as fractional values. Estimated errors in the last significant figures of the experimental data are given in brackets.

	Experimental			DFT		
Atom	x	y	z	x	y	z
C1	0.5877(3)	0.1211(3)	0.7187(3)	0.5870	0.1215	0.7130
C2	0.4629(3)	0.2689(2)	0.6755(4)	0.4588	0.2671	0.6644
C3	0.2890(3)	0.2172(3)	0.7044(3)	0.2834	0.2135	0.6960
N4	0.6866(2)	0.0051(2)	0.7463(3)	0.6917	0.0080	0.7490
N5	0.1476(2)	0.1770(2)	0.7258(3)	0.1418	0.1750	0.7167
H6	0.4588(6)	0.3152(6)	0.4992(5)	0.4531	0.3104	0.4866
H7	0.5106(6)	0.3847(5)	0.7845(7)	0.5037	0.3836	0.7740

3.2. Crystal structures

The relaxed crystal structure of δ-malononitrile calculated by DFT is reported with the experimental results in table 1. The two calculated lattice parameters agree with the experimental data with an underestimate of 2.6% in both cases. We remark that the experimental data are not for low temperature so there will be an effect of thermal expansion, which could reasonably account for some of the discrepancy.‖ We also compare the experimental (5 K) and DFT-calculated crystal structures of the α phase in Table 3. For the α phase, the calculated values are in closer agreement with experimental data (maximum error 1%). Experimental and calculated bond lengths and angles calculated for the δ and α phases are compared in table 2. Bond lengths agree to within experimental data. Note that the DFT calculations give a distance of 2.28 Å for the lengths of the hydrogen bonds in the δ phase, shorter than the experimental value (given above) of around 8%, and which is consistent with the shorter lattice parameters calculated by DFT.

3.3. Elasticity

The elastic properties of the α and δ phases were obtained by performed energy minimisation calculations for a range of pressures 0–3 GPa and fitting the $V(P)$ data to the third-order Birch–Murnaghan isothermal equation of state. The results gave bulk modulus values of 3.0 and 3.4 GPa for the α and δ phases respectively, with values of its derivative of 3.0 for both phases. The higher elasticity of the δ phases 13% greater than that of the α phase) is in spite of the fact that the δ phase at a temperature of 260 K

‖ We investigated whether any factors such as sample displacement in the experiment might account for the larger values of the lattice parameters, but including additional factors in the refinement reduced the difference between refined values and those calculated here by no more than 2%.

Table 4. Decomposition of the phonons modes for the α and δ phases of malononitrile.

	α phase	δ phase
Total:	$21A_g + 21A_u + 21B_g + 21B_u$	$10A_1 + 10A_2 + 10B_1 + 10B_2 + 22E$
Internal:	$15A_g + 15A_u + 15B_g + 15B_u$	$8A_1 + 8A_2 + 8B_1 + 8B_2 + 14E$
External optic:	$5A_g + 6A_u + 6B_g + 4B_u$	$A_1 + 2A_2 + 2B_1 + 2B_2 + 7E$
Acoustic:	$A_u + 2B_u$	$A_1 + E$

has lower density (6% lower, data from the previous neutron scattering measurements [5]). This presumable reflects the stiffening of the structure by the hydrogen bonds.

3.4. Long-wavelength optic phonons

The decompositions of the long-wavelength phonons of both the α and δ phases into the sets of irreducible representations are given in table 4. Here we separate the internal molecular vibrations from the lower-frequency vibrations which predominantly consist of translations and rotations of molecules, and which we call the external modes. The calculated vibrational frequencies for internal modes for the α and δ phases are reported in table 5. The data for the α phase are compared with the detailed spectroscopic measurements of Castellucci and Manzelli [23] obtained in the identical γ phase; data from polycrystalline phases by Le Calvé et al [24] and Savoie et al [10] are consistent with the single-crystal data. The agreement between the DFT calculations and spectroscopic data are generally good.

The calculated external mode frequencies are given in table 6. All the Raman frequencies for the α phase at a temperature of 15 K have been measured by Le Calvé et al [24] and are given in this table for comparison. Infrared spectroscopic data for the α phase have been reported by Savoie et al [10] and are included in table 6. Savoie et al [10] have reported both Raman and Infrared spectroscopic data for some external modes of the δ phase and these are also reported in table 6. In all cases the agreement is reasonable.

The agreement (or perhaps, lack of any significant disagreement) between the calculated and measured Raman and Infrared spectroscopy data add strong support to the proposed crystal structure of the δ phase of malononitrile.

3.5. Phonon dispersion curves

Phonon dispersion curves for the α and δ phases for selected directions of wave vectors in reciprocal space and frequencies in the range 0–6 THz are shown in figure 5. Although the structures of the two phases are different, the dispersion curves show some similarities. In both cases the top four branches, with frequencies between 5–6 THz, are the lowest-frequency internal modes, corresponding to the $C(CN)_2$ scissor mode, one per molecule. These branches do show some variation of frequency with wave vector, and in the δ phase they are more closely bunched together whereas in the α phase these internal modes

Table 5. Calculated internal molecular vibrational frequencies (units cm^{-1}) for the α and δ phases of malononitrile, compared with the extensive set of measurements on a single crystal sample of the monoclinic γ phase at 298 K by Castellucci and Manzelli [23].

DFT α phase				Spectroscopy γ phase				DFT δ phase				
A_g	B_g	A_u	B_u	A_g	B_g	A_u	B_u	A_1	A_2	B_1	B_2	E
165	189	171	170	181	181	—	—	173	184	190	178	—
345	344	345	344	340	343	342	339	—	—	—	—	352, 355
370	369	370	371	365	365	366	366	379	—	—	379	377
380	377	373	376	373	368	372	372	—	379	380	—	379
580	579	579	581	581	578	580	581	585	587	586	583	—
887	879	883	881	895	892	892	890	886	884	886	881	—
891	888	896	898	—	936	937	938	—	—	—	—	893, 894
968	973	967	981	983	983	982	991	—	—	—	—	967, 970
1185	1185	1181	1180	1215	1213	1214	1215	1196	1202	1201	1200	—
1279	1275	1275	1293	1310	1308	1309	1322	—	—	—	—	1290 1295
1361	1362	1348	1346	1391	1386	1393	1387	1347	1354	1350	1356	—
2264	2265	2266	2264	2264	2272	2266	2271	—	—	—	—	2263 2263
2270	2273	2273	2271	2291	2291	2292	2288	2267	2271	2270	2272	—
2938	2941	2938	2937	2928	2930	2932	2929	2909	2918	2909	2919	—
2991	2993	2994	2994	2965	2966	2967	2966	—	—	—	—	2958, 2959

appear to be in two groups with slightly different frequency. There are 24 external modes, which in both phases are distributed up to around 5 THz. Similarly the top frequencies of the acoustic modes are similar in both phases, at around 1.3–1.8 THz.

One striking difference between the phonon spectrum of the two phases is that the lowest-frequency optic mode in the δ phase are at around 2 THz, but are at around 1 THZ in the α phase. The lowest frequency optic mode in the α phase has B_g symmetry, and is the soft mode for the α–β displacive phase transition, as has been measured by Raman scattering as functions of temperature at ambient and elevated pressures [24, 7]. We have calculated this frequency as a function of pressure, showing a clear softening of the B_g mode as a function of pressure, with the frequency reaching zero at a pressure of 1.06 GPa. Qualitatively this reflects the experimental situation, where at low temperature the soft mode induces the α–β phase transition albeit at the lower pressure of 0.32 GPa by extrapolation. The over-estimate of the phase transition pressure is not uncommon for DFT calculations, particularly in view of the approximate treatment of the dispersion interaction and consistent with the known effects of the approximate nature of the DFT functionals. We also remark that in the dispersion curves, figure 5, the soft mode appears to soften mostly around zero wave vector rather than across the whole dispersion curve. On increasing pressure this becomes more apparently, with

Table 6. Calculated external vibrational frequencies (units cm^{-1}) for the α and δ phases of malononitrile, compared with spectrosopic measurements. The IR absorption spectroscopy data in both phases and the Raman scattering data for the δ phase are taken from Savoie et al [10], and the Raman scattering data for the α phase are taken from Le Calvé et al [24]

α phase				δ phase			
	DFT	Raman	IR		DFT	Raman	IR
B_g (R)	27	13		B_2 (R)	62	50	
A_g (R)	59	59		E (R,IR)	71		68
B_u(IR)	69		69	A_1 (R,IR)	72		77
A_u(IR)	71		74	A_2	80		
A_g (R)	71	69		E (R,IR)	104	90	
A_u(IR)	84		79	E (R,IR)	107		100
A_g (R)	87	80		B_1 (R)	108		
B_g (R)	96	93		E (R,IR)	111	115	
A_g (R)	105	98		E (R,IR)	129	126	
A_u(IR)	113		107	A_2	133		
B_g (R)	112	104		E (R,IR)	136		138
B_u(IR)	114			B_1 (R)	137		
B_g (R)	118	110		B_2 (R)	145	142	
A_g (R)	124	113		E (R,IR)	149		146
B_g (R)	128	124					
A_u(IR)	134		126				
B_u(IR)	135						
B_u(IR)	141						
A_g (R)	142	136					
B_g (R)	146	150					
A_u(IR)	150						

softening only occurring at zero wave vector and not at the Brillouin zone boundaries.

The comparison between the phonon spectra of the α and δ phases is highlighted in the calculation of the phonon density of states at zero pressure, as shown in figure 6. This was constructed from calculations of the phonon frequencies at 500 random wave vectors in each phase. The difference in the distribution of external modes for frequencies in the range 5–6 THz described above can be seen as a single peak in the density of states for the δ phase and as two peaks for the α phase. The other clear difference is that there is an enhancement in the number of modes between 1–2 THz in the α phase as highlighted in the phonon dispersion curves in the regime of the soft mode. The importance of this difference will be discussed below.

One final remark is that we searched for additional softening of phonons under pressure as precursors of the phase transition to the high-pressure phase [7]. However, calculations at all the symmetry points on the surface of the Brillouin zone of the α phase failed to show any significant phonon softening up to a pressure of 3 GPa.¶ This

¶ Strictly speaking the transition is from the lower-symmetry β phase, but we can reasonably expect that we should see the same instability in the α phase given that the soft modes for the α–β phase

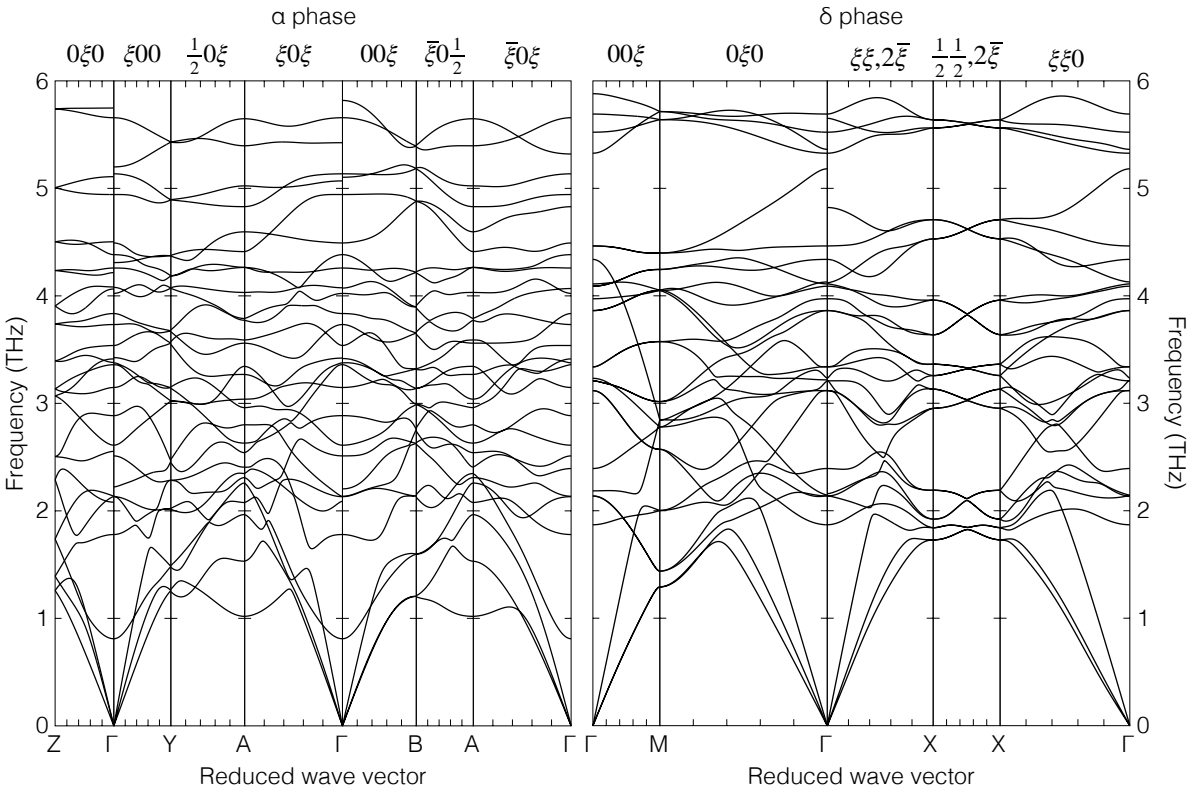

Figure 5. Lower-frequency dispersion curves of the α phase (left) and δ phase (right) of malononitrile calculated by DFT as described in the text. The Brillouin zone labels in the α phase as given by the Bilbao Crystallographic Server [25] are $\Gamma = (0, 0, 0)$, $Z = (0, 0, 0.5)$, $Y = (0.5, 0, 0)$, $A = (\pm 0.5, 0, 0.5)$, and $B = (0, 0, 0.5)$. The Brillouin zone labels in the δ phase are $\Gamma = (0, 0, 0)$, $M = (0, 0, 1)$, and $N = (0.5, 0, 0.5)$.

may be rather surprising since the experimental evidence suggests the transition is of displacive kind [7].

3.6. Calculations of lattice energy and phonon free energy

The optimised lattice energies (no vibrational energy) of the two phases show that the value for the δ phase is lower than that for the α phase by 1.77 kJ/mol. Experimentally this difference at 260 K been determined as 1.26 kJ/mol [3]. Given the approximations within DFT, and the use of approximations in the dispersion interaction, the calculation of this small energy difference is satisfactory.

We have calculated thermodynamic functions of the α and δ phases from a phonon calculation using the same set of random set of 500 wave wave vectors as used in the calculation of phonon density of states. The phonon entropy curves calculated from the phonon frequencies used in the density of states are shown in figure 7, and compared with experimental data [3]. As expected, the α phase has a higher entropy at each

transition and β to high-pressire phase transition will have different symmetry and thus no low-order coupling.

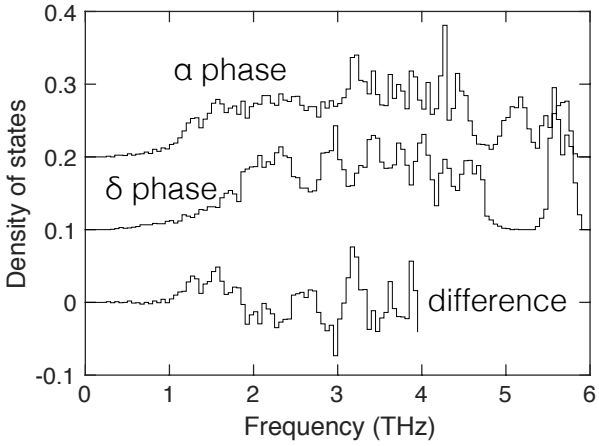

Figure 6. Phonon densities of states for the α phase (top curve) and δ phase (middle curve) of malononitrile calculated by DFT, with the bottom curve showing the difference between the two at low frequencies.

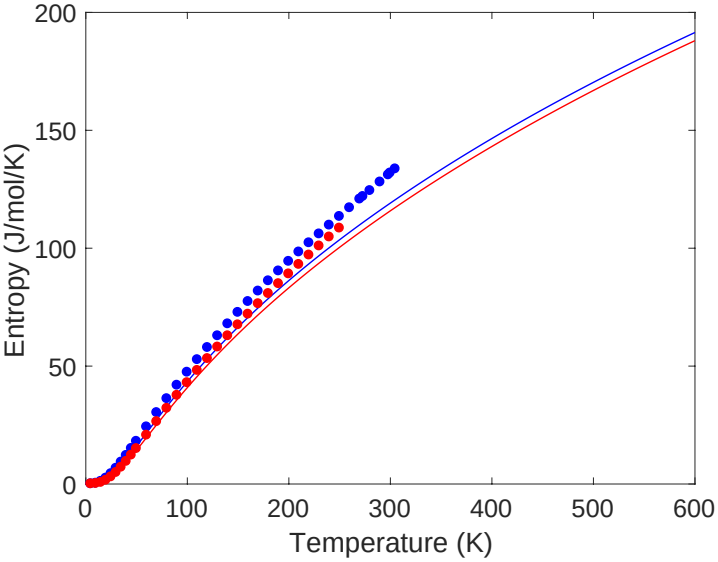

Figure 7. Calculated entropies of the α (top continuous curve, blue) and δ (lower continuous curve, red) phases of malononitrile, compared with the experimental data [3] shown as filled circles with corresponding colours.

temperature, consistent with having a higher zero-temperature energy and thus required for the existence of the phase transition to the β/γ phases at temperatures above 260 K. The calculated values of the entropies of the two phases correspond reasonably well to the experimental measurements, albeit with the experimental entropies being slightly higher. For example, at the temperature of 120 K the calculated values of entropy of the α and δ phases are 53.2 and 50.5 J/mol/K respectively, with corresponding experimental values of 57.8 and 53.1 J/mol/K [3]. The discrepancy, aside from small inherent errors in the DFT calculations, is likely to be exacerbated by not taking into account the effects of thermal expansion in the calculation, and in the case of the α phase also by neglecting

the effect of the phase transitions in lowering of the frequencies of the phonons associated with the soft mode on heating, consistent with the fact that the larger discrepancy is for the α phase.

The free energies of the α and δ phase were constructed from the lattice energy and entropy. Their curves cross – the point of the phase transition – at a temperature of 567 K, which is more than twice the actual phase transition temperature of 260 K. If the full free energy curves are made to cross at the experimental transition temperature we need an energy difference of 0.697 kJ/mol. However, since this is around half the experimental energy difference, it is probably the case that the mismatch between the experimental and theoretical transition temperature is mostly due to the underestimate of the entropy difference, again by around a factor of 2.

4. Conclusion

This paper has reported the last unknown information concerning the ambient-pressure phase transitions in the molecular crystal malononitrile, namely the crystal structure of the δ phase, following the recent report of the crystal structure of the α phase and of the temperature dependence of the crystal structure through the α–β–γ re-entrant sequence of phase transitions. The crystal structure of the δ phase appears to be consistent with previous experimental data, including the empirical observation that the transition into the δ is accompanied by a significant volume increase [3]. The phase transition to the δ phase is reconstructive rather than displacive type, which is most clearly seen through changes in C–H...N bonding.

DFT calculations of the lattice energies and lattice dynamics have expanded the picture and confirmed that the zero-temperature energy of the δ phase is lower than that of the α phase, and that the entropy of the α phase is higher, both of which are consistent with the existence of the reconstructive transition between the two phases. The DFT calculations show that the origin of the extra entropy in the α phase is associated with the low-frequency soft mode associated with the α–β–γ phase transitions, and the softening of this mode to zero frequency has been seen in the calculations performed with different pressures. The key finding of this work is that the existence of the α–β–γ phase transitions have directly given these phases the stability over the lower-energy δ phase at high temperatures as an entropic effect. In the study of organic polymorphism, it is known that many potential different crystal structures may have similar energies, and in thus the entropic contribution to the free energy is important.

The main remaining question regarding the phase transitions of malononitrile concerns the crystal structure of the high-pressure phase [7]. Surprisingly no onset of this phase transition could be seen through any pressure-induced instabilities in the phonon spectrum.

5. Postscript: a brief personal reflection

This paper has been written towards the close of the career of the corresponding author, and the main topic of this paper, the phase transitions in the molecular crystal of malononitrile, was also the topic of his PhD thesis [4, 9, 26, 27]. Gratifyingly this paper now answers some of the questions left unanswered by that and subsequent works, up to a new analysis of the crystallography of the α–β–γ phase transitions [5]. Given that the topic of this paper spans the larger part of a scientific career, it is interesting to reflect on three significant differences between then and now. First is the use of computer graphical visualisation of crystal structures. From figure 4 it is easy to quickly see the change in the hydrogen-bonding network, but back in the early 1980s such structures had to be drawn by hand, as in earlier references [4, 26].[+] Second is the considerably-enhanced capability of the Rietveld method, as highlighted in our study of the α–β–γ phase transitions [5]. The Rietveld refinements reported here were carried out within seconds as an interactive task, but during the PhD of the corresponding author, Rietveld analysis could only be performed as batch jobs with each cycle of refinement lasting several minutes, and with rather lower capabilities (such as the restriction of having a linear sloping background functions, and fitting to a single histogram of data). Third is the massive developments in computer modelling seen over this period of time. In the 1980s we were restricted to calculations with empirical potentials [26], and to a large extent researchers had to write their own modelling programs.[*] The capability to perform accurate ab initio calculations of phonon spectra for such systems is truly impressive. All of these developments reflect the exponential increased in computer capability over the past 40 years, and looking back over a career it seems that it is the computer that both gives the potential for many exciting developments and which now determines the rate of progress.

Acknowledgments

MTD is grateful to Dr Alan Hewat of the ILL for support during the neutron diffraction experiment. He is also grateful to Dr Mark Johnston of the ILL for help in retrieving the data from the ILL archives. Furthermore, MTD is also grateful to his mentors at the time of the original data collection and before, Prof Stuart Pawley (Edinburgh) and Dr Alastair Rae (Birmingham) respectively. LT is grateful to the China Scholarship Council and Queen Mary University of London for financial support. Calculations were performed on two computing resources, which we are pleased to acknowledge. First was ARCHER UK National Supercomputing Service, with time obtained through our membership of the UK's HEC Materials Chemistry Consortium, which is funded by

[+] As a young post-doctoral researcher, and inspired by a television programme regarding the future of science, he naively asked his computer centre whether software for drawing atoms inside crystals yet existed, only to be reminded that he had been inspired by the future and not present capabilities!

[*] Indeed, the corresponding author had to write his own lattice energy minimisation program during his PhD work [9, 26].

EPSRC (EP/L000202, EP/R029431). Second was the HPC Midlands Plus tier-2 system as consortium members, also supported by EPSRC (EP/P020232/1).

References

[1] Sussman A and Alexander S 1967 Nuclear quadrupole resonance study of critical behaviour in malononitrile. *Solid State Commun.* **5** 256–62

[2] Sussman A and Alexander S 1968 Displacive phase transitions in malononitrile. *J. Chem. Phys.* **49** 3792

[3] Girdhar H L, Westrum E F and Wulff C A 1968 Thermodynamic properties and 3rd-law cycle for malononitrile. *J. Chem. Eng. Data* **13** 239–242

[4] Dove M T and Rae A I M 1980 Structural phase transitions in malononitrile. *Faraday Discussions* **69** 98–106

[5] Dove M T 2011 The re-entrant phase transitions in crystalline malononitrile, $CH_2(CN)_2$: a neutron powder diffraction study. *J. Phys.: Condens. Matter* **23** 225402

[6] Levitskii R R, Andrusyk A Y and Zachek I R 2010 Dynamics of the Rochelle salt $NaKC_4H_4O_6.4H_2O$ crystal studied within the Mitsui model extended by piezoelectric interaction and transverse field. *Condensed Matter Physics* **13** 13705

[7] Krauzman M, Pick R M, Le Calvé N and Pasquier B 1983 Raman spectra and reentrant phase diagram of malononitrile $CH_2(CN)_2$. *J. Physique* **44** 849–858

[8] Chanh N B, Haget Y, Le Calvé N, Novak A and Pasquier B 1981 Polymorphism of malononitrile. Crystallographic characterization of the L–F phase transition. *J. Appl. Cryst.* **14** 1–2

[9] Dove M T 1982 The structural phase transitions in the molecular crystal malononitrile. Unpublished PhD thesis, University of Birmingham

[10] Savoie R, Brousseau R and Nolin C 1976 Vibrational spectra of crystalline malononitrile. *Canadian Journal of Chemistry* **54** 3293–302

[11] LeBail, A 2005. Whole powder pattern decomposition methods and applications: a retrospection. *Powder Diffraction* **20** 316–326

[12] Hewat A W and Bailey I 1976 D1A, a high resolution neutron powder diffractometer with a bank of mylar collimators. *Nucl. Instrum. Methods* **137** 463–71

[13] Larson A C and Von Dreele R B 2000 General Structure Analysis System (GSAS), *Los Alamos National Laboratory Report LAUR 86-748*

[14] Toby B H 2001 EXPGUI, a graphical user interface for GSAS. *J. Appl. Cryst.* **34** 210–3

[15] Caglioti G, Paoletti A and Ricci F P 1958 Choice of collimators for a crystal spectrometer for neutron diffraction. *Nuclear Instruments and Methods* **3** 223–8

[16] Palmer D C 2015 Visualization and analysis of crystal structures using CrystalMaker software. *Zeitschrift für Kristallographie* **230** 559–72

[17] Clark S J, Segall M D, Pickard C J, Hasnip P J, Probert M J, Refson K and Payne M C 2005 First principles methods using CASTEP. *Zeitschrift für Kristallographie* **220** 567–70

[18] Grimme S 2006 Semiempirical GGA-type density functional constructed with a long-range dispersion correction. *J. Comput. Chem.* **27** 1787–1799

[19] Refson K, Clark A J and Tulip P R 2006 Variational density functional perturbation theory for dielectrics and lattice dynamics. *Physical Review B* **73**155114

[20] Perdew JP, Burke K, Ernzerhof M 1996 Generalized Gradient Approximation Made Simple. *Phys. Rev. Lett.* **77** 3865–3868

[21] Monkhorst H J, Pack J D 1976 Special points for Brillouin-zone integrations. *Phys. Rev. B* **13** 5188–5192

[22] Rimmer L H N, Dove M T 2015. Simulation study of negative thermal expansion in yttrium tungstate $Y_2W_3O_{12}$. *J. Phys.: Condens. Matter* **27** 185401

[23] Castellucci E and Manzelli P 1975 The infrared and Raman spectra of malononitrile single crystal at 25°C. *Chemical Physics* **9** 135–45

[24] Le Calvé N, Pasquier B and Novak A 1980 Vibrational study of phase transition of solid malononitrile. *J. Chem. Phys.* **72** 6409–13

[25] Kroumova E, Aroyo M I, Perez-Mato J M, Kirov A, Capillas C, Ivantchev S and Wondratschek H 2003 Bilbao Crystallographic Server: Useful databases and tools for phase-transition studies. *Phase Transitions* **76** 155–170; `http://www.cryst.ehu.es/cryst/get_kvec.html`, accessed 29 November 2018

[26] Rae A I M and Dove M T 1983 A new theoretical model for the re-entrant phase transitions in malononitrile. *J. Phys. C: Solid State Phys.* **16** 3233–44

[27] Dove M T, Farelly G, Rae A I M and Wright L 1983 The re-entrant phase transitions in malononitrile: specific heat capacity measurements. *J. Phys. C: Solid State Phys.* **16** L195–8